Theory and Practice of Science and Technology
2025, VOL. 6, NO. 10, 66-71
DOI: 10.47297/taposatWSP2633-456913.20250610

Prediction of Rolling Deformation Using a Bayesian-Optimized BP Neural Network

Guoqing Qiao[1,2], Qiansong Zhang[1,2]

[1]School of Mechanical Engineering, Tianjin University of Technology and Education, Tianjin 300222, China

[2]Tianjin Key Laboratory of Intelligent Robot Technology and Application Enterprise, Tianjin, 300222, China

ABSTRACT
To address the challenge of accurately evaluating the relationship between roller burnishing parameters and surface deformation in ultra-high strength steel torsion bars, this paper develops a Bayesian-optimized neural network model incorporating physical constraints. The model features a dual-output channel architecture that simultaneously predicts the rolling diameter variation and outputs a variance reliability metric, enabling quantitative assessment of prediction uncertainty. By integrating Bayesian optimization for global hyperparameter tuning, along with the SiLU activation function and a composite physical constraint loss function containing second derivatives, the model significantly enhances generalization capability and prediction accuracy through a triple-control mechanism. Experimental results demonstrate that the model reduces the mean absolute error of rolling diameter variation prediction to 0.051 μm, while its variance warning mechanism effectively identifies anomalous inputs beyond processing parameter ranges (e.g., 9000 N rolling force), enabling dynamic evaluation of prediction reliability. This approach provides valuable technical support for high-performance and high-precision intelligent manufacturing of spring torsion bars.

KEYWORDS
Rolling; Bayesian optimization; neural network; torsion bar; deformation

1 Introduction

Torsion bars, as critical load-bearing components for transmitting torque, are highly susceptible to fracture under long-term alternating stresses [1]. Roller burnishing, as a surface strengthening process, enhances fatigue performance by introducing beneficial residual compressive stress. The resulting macroscopic dimensional changes caused by residual stress can serve as an evaluation indicator for process effectiveness [2]. Consequently, the dimensional variation of the torsion bar's outer circle can be used as a substitute evaluation parameter. However, in practical production environments, torsion bars possess complex structures and undergo minimal deformation (approximately 20 μm). Traditional measurement methods suffer from limitations such as low efficiency, high cost, and potential damage to the workpiece.

To address these issues, artificial neural networks (ANNs) have been introduced into the field of deformation prediction. For instance, Lü Xiaodan et al [3]. successfully employed a BP neural network to predict the elastic deformation of composite steel structures. To further improve the accuracy of prediction models, researchers have incorporated optimization algorithms to enhance network performance. Zeng Quan et al [4]. in their study on residual stress prediction in GH3625 superalloy, systematically compared various network models including BP and Genetic Algorithm-optimized BP (GA-BP), noting that the GA-BP neural network demonstrated superior prediction performance. Although the aforementioned studies have made progress in average prediction accuracy, existing methods still exhibit insufficient accuracy when handling complex nonlinear relationships, and simultaneously lack the capability for uncertainty quantification in their predictions.

In summary, this paper proposes a Bayesian-optimized neural network architecture with the following key innovations: (1) constructing a Bayesian optimization collaborative framework to form a closed-loop mechanism of "parameter optimization-evaluation-adaptive re-optimization"; (2) building a physics-informed dual-channel network that outputs both the predicted value μ of the rolling diameter variation and the variance estimate σ^2 (predictive reliability); (3) designing a hybrid loss function incorporating second-derivative constraints, which introduces curvature smoothing terms and process constraint terms based on traditional mean square error, ensuring the physical plausibility of the prediction results.

2 Experimental Scheme and Data Collection

To investigate the influence of roller burnishing process parameters on the diameter variation of torsion bar outer circle specimens and to provide a data foundation for subsequent neural network model training, this study adopted a three-factor, five-level experimental design (totaling 125 sets). Segmented roller burnishing experiments were conducted on a CA6140 lathe using ultra-high strength steel (45CrNiMoVA) specimens (the setup is shown in Fig. 1). Each process stage corresponded to a specific parameter combination. The collected independent variables $x_i=(F_i,f_i,n_i)$consisted of the rolling force, workpiece feed rate, and spindle speed. The dependent variable y_i was the diameter variation after burnishing. Ultimately, a dataset $\{(x_i,y_i)\}$ containing 125 data pairs was constructed.

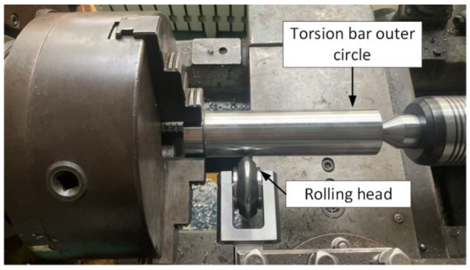

Figure 1 Roller burnishing test device

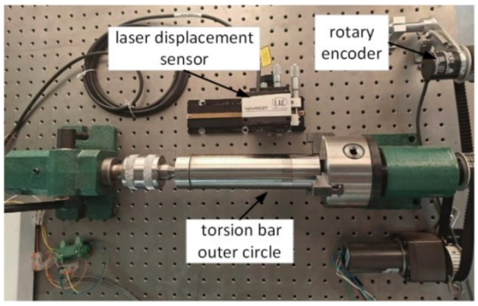

Figure 2 Rolling diameter variation measuring device

The diameter variation was measured using a well-established laser displacement sensor [8]. The burnished specimen was mounted on a dedicated acquisition setup (Figure 2), ensuring that: (1) the measurement point remained within the sensor's operating range (25 mm <L_t < 50 mm), and (2) the specimen axis was aligned horizontally with the laser head. The initial distance L_0 from the sensor to the workpiece axis was calibrated following the procedure illustrated in Fig. 3.

$$L_0=L_t+R_0 \tag{1}$$

Where R_0 is the outer circle radius of the torsion bar, and L_t is the distance from the outer circle surface to the sensor.

During measurement, the torsion bar's outer circumference rotated uniformly. The laser displacement sensor and encoder operated synchronously, recording data vectors(L_t ,θ_t) at fixed intervals, where Lt is the instantaneous surface distance and θ_t is the corresponding spindle rotation angle. These vectors were converted into polar coordinates (R_t,θ_t) using Eq. (2), where Rt represents the instantaneous radius from the workpiece surface to its axis, and L_0 denotes the pre-calibrated reference distance. Using this measurement methodology, experimental data for the rolling diameter variations were successfully obtained.

$$R_t=L_0-L_t \tag{2}$$

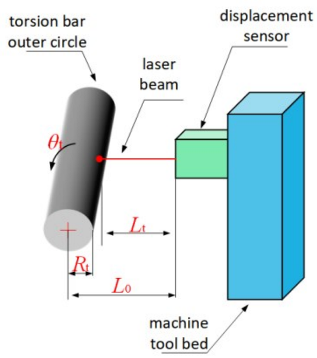

Figure 3 Schematic diagram of outer circle measurement

3 Construction of a Bayesian-Optimized Dual-Channel BP Neural Network Prediction Model

3.1 Dual-Channel Network Design

The core components include a shared feature layer, a deformation prediction layer, and a variance prediction layer. The shared layer is used to extract common features, while the dual channels achieve task differentiation through nonlinear mapping. The schematic diagram of the final network architecture is shown in Figure 4.

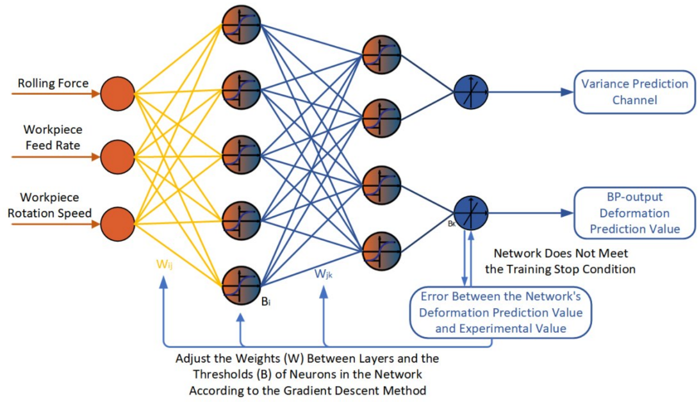

Figure 4 Schematic diagram of dual-channel network architecture

Shared Feature Layer: As the backbone of the network, this layer receives the original process parameters as input, extracts general features through nonlinear transformations, and provides a foundation for the subsequent dual prediction heads. Its computational expression is:

$$h_l = SiLU(W_l h_{l-1} + b_l), \quad l = 1,\cdots,L \tag{3}$$

Where h_0 is the original input vector, L is the total number of hidden layers, W_l and b_l are the weight matrix and bias vector of the l-th layer, respectively, and *SiLU* is the activation function.

Deformation Prediction Head: Based on the shared feature h_L, this channel outputs the rolling diameter variation μ. The expression is:

$$\mu = W_{\mu 2} \cdot \tanh(W_{\mu 1} h_L + b_{\mu 1}) + b_{\mu 2} \tag{4}$$

Variance Prediction Head: Operating in parallel with the deformation prediction head, this channel outputs the log-variance $log\sigma^2$ to quantify prediction uncertainty. The expression is:

$$\log \sigma^2 = W_{\sigma 2} \cdot \tanh(W_{\sigma 1} h_L + b_{\sigma l}) + b_{\sigma 2} \tag{5}$$

The two prediction heads share the input features but are trained with independent weight parameters, providing both the predicted value and its reliability assessment.

3.2 Bayesian Hyperparameter Optimization

To address the challenge of selecting neural network hyperparameters (e. g., number of network layers, number of neurons) [5], this study introduces a Bayesian optimization algorithm for intelligent optimization, the optimal solution can be found in the global optimization strategy with fewer iterations.

3.2.1 Hyperparameter Search Space

$$\begin{aligned} &1e-3 \le lr \le 0.1 \\ &2 \le hidden \le 20 \\ &1 \le Lays \le 4 \\ &0.1 \le Dropout \le 0.5 \end{aligned} \tag{6}$$

where lr denotes the initial learning rate, hidden is the number of neurons per hidden layer, Lays is the number of hidden layers, and Dropout is the dropout rate.

3.2.2 Optimization Formulation

The hyperparameter optimization problem is defined as:

$$\theta^* = \arg\min_{\theta \in \Theta} \mathcal{L}_{\text{val}}(\theta) \tag{7}$$

where the hyperparameter combination is denoted as $\theta \in \Theta$, and (θ) represents the validation set loss function.A Gaussian Process surrogate model is constructed as:

$$f(\theta) \sim GP\left(\mu_t(\theta), k(\theta, \theta')\right) \tag{8}$$

Improved risk-sensitive expected improvement function:

$$EI_\lambda(\theta) = E\left[\max\left(f_{\min} - f(\theta), 0\right)\right] - \lambda \cdot \sigma(\theta) \tag{9}$$

Where: the empirical adjustment factor λ=0.5, and σ(θ) denotes the predicted standard deviation. This design suppresses ineffective exploration by penalizing high-variance regions (the second term).

In summary, the Bayesian hyperparameter optimization framework can rapidly identify the optimal values of key parameters such as the learning rate and network depth while maintaining global search capability, thereby providing a stable structural foundation for the subsequent implementation of the dual-channel neural network.

3.3 Improved Loss Function

To overcome the limitations of the traditional Mean Squared Error (MSE) loss in physical modeling, which often results in predictions exceeding practical process windows or exhibiting oscillatory behavior [6], this paper introduces a composite loss function that synergistically combines probabilistic modeling with physical mechanisms. This function leverages a coordinated triple mechanism—encompassing statistical optimization, boundary constraints, and curvature smoothing—to ensure that all predictions are consistent with the principles of metal plastic deformation. The overall loss is defined as:

$$\mathcal{L}_{total} = \mathcal{L}_{nll} + \alpha \mathcal{L}_{phy} + \beta \mathcal{L}_{curv} \tag{10}$$

(1) Negative Log-Likelihood Loss: Enables dual-channel collaborative optimization, simultaneously predicting the diameter variation μ and the variance σ^2:

$$\mathcal{L}_{nll} = \frac{1}{2N} \sum_{i=1}^{N} \left(\frac{\left(y_i - \mu_i\right)^2}{\sigma_i^2} + \log \sigma_i^2 \right) \tag{11}$$

where N is the number of samples, and the balance factors are α=0.3 and β=0.2.

(2) Physical Constraint Term: Applies boundary constraints to the standardized rolling force F using the *ReLU* function:

$$\mathcal{L}_{phy} = \frac{1}{N} \sum_{i=1}^{N} \left[\mathrm{Re}\,LU\left(F_i - 8.0\right) + \mathrm{Re}\,LU\left(4.0 - F_i\right) \right] \tag{12}$$

The original rolling force F ∈ [4000, 8000] N is linearly mapped to the range [4.0, 8]. Penalties are triggered when F falls outside this interval.

(3) Curvature Constraint Term: Suppresses non-physical oscillations in the prediction surface via second-order derivatives:

$$\mathcal{L}_{curv} = \frac{1}{N} \sum_{i=1}^{N} \left(\left\| \frac{\partial^2 \mu}{\partial F^2} \right\|_2 + \left\| \frac{\partial^2 \mu}{\partial f^2} \right\|_2 \right) \tag{13}$$

Second-order derivatives with respect to the rolling force F and the feed rate f are computed using automatic differentiation (Autograd), ensuring smooth variation of the predicted output with process parameters.

In summary, the construction of this dual-channel neural network first determines the optimal hyperparameter combination via Bayesian optimization, then completes model training using the improved composite loss function.The trained model can simultaneously output the predicted value of the rolling diameter variation and its variance,with the overall flowchart shown in Figure 5.

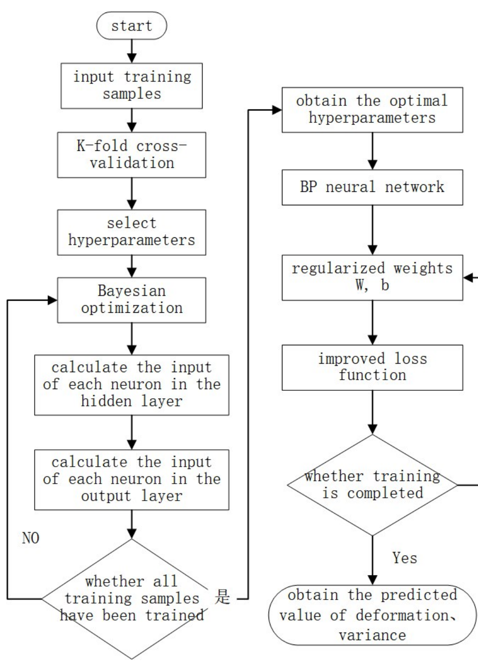

Figure 5 Flowchart of the Bayesian optimized dual-channel BP neural network prediction model framework

4 Experimental Analysis

To ensure the accuracy of model training and evaluation, this study adopts K-fold cross-validation (with K = 5) for dataset partitioning. Specifically, the original dataset is randomly divided into K subsets of approximately equal size. In each of the K iterations, K-1 subsets are selected as the training set, while the remaining 1 subset serves as the test set.

4.1 Bayesian Optimization Process

Figure 6 demonstrates the effective optimization performance of the Bayesian optimization process. Over 50 iterations, the algorithm rapidly reduced the total loss function from an initial value of 0.09 to 0.012. Through extensive exploration, it effectively avoided local optima, resulting in a clear stepwise decline in the optimal loss, which eventually stabilized and converged to a low level of approximately 4.662×10^{-5}.

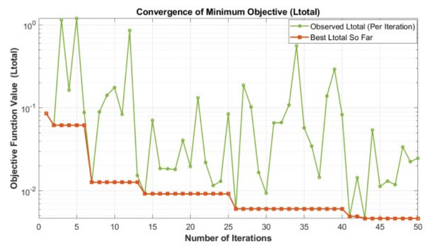

Figure6 The iterative process and results of hyperparameter optimization

After determining the hyperparameters for the BP neural network using the Bayesian optimization method (final values in Table 1), a prediction model was constructed and trained based on this optimal combination, and its performance was subsequently verified and analyzed in detail.

Table.1 Optimal combination of hyperparameters

Parameter Name	Parameter Setting
Learning Rate (lr)	0.001
Dropout	0.3
Neurons (hidden)	16
Layers (Lays)	3

4.2 Predictive Performance Comparison

The Mean Absolute Error (MAE) and the Coefficient of Determination (R^2) were adopted as model evaluation metrics.

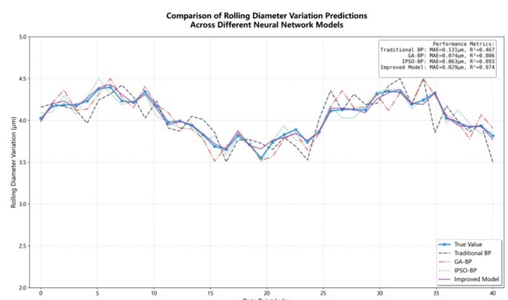

Figure 7 A comparison chart between the predicted value and the true value

To verify the performance advantage of the improved model, 40 data points were randomly selected from the dataset for testing. As shown in Figure 7, among the four compared algorithms, the prediction curve of the improved model (purple dashed line) matches the true values (blue solid line) most closely, significantly outperforming the other methods. Its quantitative evaluation metrics are MAE = 0.051 and R^2 = 0.959, indicating that the model possesses high prediction accuracy and reliability.

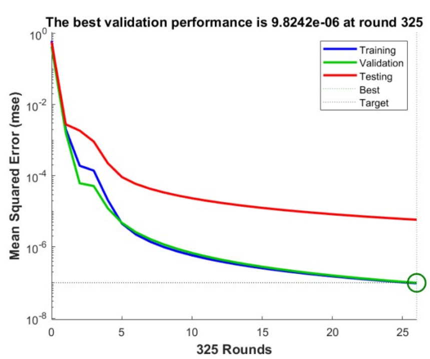

Figure 8 Convergence curve of loss function

The model's training process and predictive performance are shown in Figures 8. The loss function curve in Figure 8 indicates that the losses of the training, validation, and test sets decreased rapidly and synchronously, stabilizing at a very low value (9.8242×10^{-6}) after 325 iterations, demonstrating that the model possesses good generalization capability without overfitting. These results collectively verify that the model achieves high predictive accuracy and stability.

4.3 Variance Early Warning Effect

To verify the effectiveness of the proposed dual-channel neural network, Figure 9 illustrates its prediction performance for rolling diameter variation on the test set and its early warning capability for abnormal operating conditions.

Results show that under normal operating conditions, the model's predicted values (red dashed line) are highly consistent with the true values (blue solid line). However, in the artificially set abnormal regions (gray background, near data points 35–45 and 75–85), the variance output increases significantly and exceeds the threshold (0.50), successfully triggering an early warning and accurately identifying two types of abnormal patterns: "excessive rolling force" and "excessive feed rate."

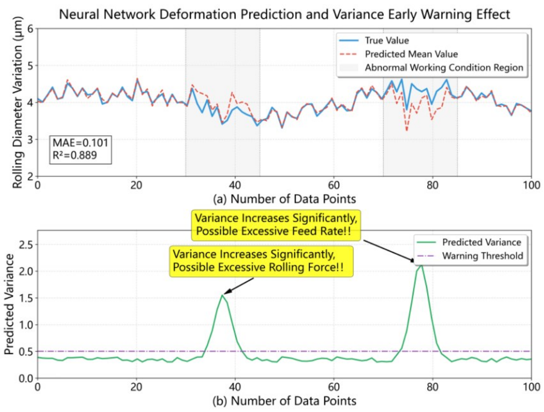

Figure 9 Variance early warning effect diagram

5 Conclusion

Addressing the issues of time-consuming measurement and high costs associated with the micron-level rolling diameter variation of ultra-high strength steel torsion bars after outer circle roller burnishing, this study successfully constructed and validated a Bayesian-optimized dual-channel neural network architecture incorporating physical mechanisms.

The model innovatively employs a dual-channel topology, which not only achieves high-precision prediction of rolling diameter variation (with a mean absolute error of 0.051μm) but also overcomes the limitation of traditional models in quantifying predictive uncertainty. Its unique variance early-warning mechanism enables real-time monitoring of prediction stability, promptly issuing alerts when processing parameters deviate from normal ranges, thereby effectively preventing potential quality risks. This intelligent analysis system, which seamlessly integrates "accurate prediction, confidence assessment, and anomaly warning," not only significantly enhances prediction reliability but also provides an innovative solution for precision control and quality assurance in high-end equipment manufacturing, showcasing broad prospects for engineering applications.

About the Author

Guoqing Qiao, a master's degree candidate, specializes in robot systems and control as well as deep learning.

References

[1] Liu Yue, Liu Hao. Investigate on low-cycle fatigue of shaft based on strain damage[J]. Manufacturing Technology & Machine Tool, 2020, (12): 55-58.

[2] Rossini N S, Dassisti M, Benyounis K Y, et al. Methods of measuring residual stresses in components[J]. Materials and Design, 2012, 35:572-588.

[3] Lü Xiaodan, Gao Shanfeng. Prediction and Simulation of Elastic Deformation of Composite Steel Structures under Non-Uniform Stress[J]. Computer Simulation, 2024, 41(08):466-470.

[4] Zeng Quan, Li Xin, Wang Kelu, et al. Study on residual stress prediction of SLM GH3625 high temperature alloy based on GA-BP and PSO-BP neural networks[J]. Journal of Plasticity Engineering, 2024, 31(03):193-199.

[5] Liu Chenhui, Zhang Weimin, Xue Feng. Research on kinematic parameters optimization of robot armbased on random forest Bayesian optimization[J]. Manufacturing Technology & Machine Tool, 2023, (01):83-90.

[6] Yang Haiyan, Hu Xincheng, Cai Jiawen, et al. Temperature prediction model for coal spontaneous combustion based onBayesian optimization support vector regression[J/OL]. Industry and Mine Automation, 1-10[2025-07-29].